

Analyse the Important Fitted Parameters Using Pulsed Fitting and Continuous CEST Approximation for Pulsed CEST

Yee Kai Tee¹, Alexandr A Khrapichev², Nicola R Sibson², Stephen J Payne¹, and Michael A Chappell^{1,3}

¹Department of Engineering Science, Institute of Biomedical Engineering, University of Oxford, Oxford, Oxfordshire, United Kingdom, ²Department of Oncology, CR-UK/MRC Gray Institute for Radiation Oncology & Biology, University of Oxford, Oxford, Oxfordshire, United Kingdom, ³Oxford Centre for Functional MRI of the Brain, University of Oxford, Oxford, Oxfordshire, United Kingdom

Introduction: Chemical exchange saturation transfer (CEST) imaging is a novel method that may offer diagnostic advantages in stroke [1] and cancer [2]. There are two types of CEST imaging – continuous CEST (CC) and pulsed CEST (PC), which are differentiated by the RF irradiation scheme used. CC uses a single long rectangular pulse [3] whereas PC employs multiple high intensity but short duration pulses to perform the saturation. Due to the specific absorption rate (SAR) and hardware limitations, CC is not feasible in clinical applications making PC the only viable irradiation scheme for the translation. However, solving the time-varying irradiation pulse MR behaviour for model fitting of PC data (pulsed fitting - PF) is time consuming since no closed-form analytical solution exists to the Bloch-McConnell model. As a result, PC is typically treated as CC by finding an equivalent average field (AF)[4] or power (AP)[5] to exploit the simple solution available for CC. In this study, numerical simulation and *in vitro* data were used to compare the results obtained by solving the time-varying irradiation pulses and using both the AF and AP approximation, when performing model-based analysis of CEST spectra.

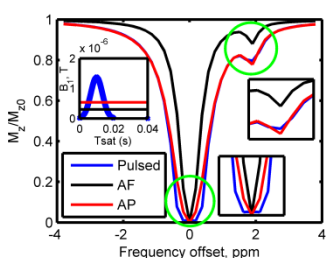


Fig. 1: Z-spectra generated using pulsed method, AF and AP approximation.

Santa Clara, CA, USA), with field of view = 80 mm x 80 mm, matrix size = 64 x 64, slice thickness = 1 mm, bandwidth = 250 kHz, TE/TR = 20/15000 ms. The saturation frequencies and the properties of the Gaussian pulses used were identical to the simulation. Echo Planar Imaging (EPI) readout was used after the saturation and the CEST data were acquired in 5 min 37 s. T_1 and T_2 of water maps were acquired according to [4]. All the data processing was done in MATLAB (Mathworks, Natick, MA, USA). A three-pool model (water (a), amide (b) and MT pool (c)) was used. Since it was not easy to separate the effect of C_b and M_{b0} [8], the latter was only permitted to change within $\pm 5\%$ of the values expected from the literature [4, 7]. For the PF, each Gaussian pulse was discretized into 32 segments for the model fitting. The other variables were assumed to be constant: $T_{1,b} = 1$, 0.0085 s [7], $T_{lc} = 1$ s [5] and T_{la} was determined using the measured values. The measured data were fitted using PF and CC approximation. The important fitted parameters using the different approaches such as water centre frequency shift, ω_a , (unavoidable) and C_b (related to pH) were analysed.

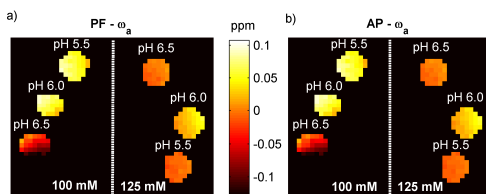


Fig. 3: Fitted ω_a using a) PF and b) AP approximation.

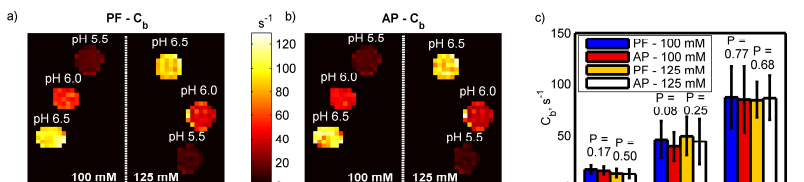


Fig. 4: Fitted C_b using a) PF and b) AP approximation, and c) across different pH and concentration phantoms. P values on top of the bars are for the two-tailed t-test.

[9], which predominantly collects samples around ω_a and the chemical shift of the amide protons, is used, PF would have to be applied because these areas produce the largest difference between the PF and AP spectra (fig. 1 and 2a). As shown in [6], when the exchange rate increases, the difference between the CEST ratio (CESTR) of CC and PC become bigger. Therefore, PF may be needed when PARCEST agents with high exchange rates are to be quantified using a model-based approach.

References: 1. Zhou *et al.*, Nat. Med. 9:1085-1090, 2003. 2. Zhou *et al.*, Nat. Med. 17:130-134, 2011. 3. Woessner *et al.*, MRM 53:790-799, 2005. 4. Sun *et al.*, MRM 60:834-841, 2008. 5. Zu *et al.*, MRM 66:1100-08, 2011. 6. Sun *et al.*, MRM 66:1042-48, 2011. 7. Sun *et al.*, MRM 59:1175-1182, 2008. 8. Sun *et al.*, JMR 202: 155-161, 2010. 9. Tee *et al.*, 19th ISMRM p. 4491, 2010.

Methods: Simulation study. A 2-pool Bloch-McConnell model (water + amide protons) was used to simulate the z-spectra of creatine phantoms (chemical shift at 1.9 ppm) generated using CC and PC. Assuming a 4.7 T scanner and saturation time of 2 s were used in the CEST experiment. For the PC, Gaussian pulses with flip angle of 180° and a 50 % duty cycle were applied from -3.8 to 3.8 ppm with increments of 0.19 ppm. Each pulse was 20 ms long and discretized into 1024 segments. To model the PC, the analytical solution of CC was used to propagate the magnetization through each discrete interval, the final values of one interval serving as the initial conditions for the next one. Crusher gradients during the interpulse delay were modelled by setting the transverse magnetization to zero. The equivalent AF and AP of the Gaussian pulses were calculated using the following formulae [5]: $AF = 1/t * \int_0^t B_1 dt$; $AP = (1/t * \int_0^t B_1^2 dt)^{-2}$, where t is the pulse duration (a Gaussian pulse + delay) and B_1 is the RF amplitude. The remaining variables used were $T_{1a,b} = 3, 1$ s, $T_{2a,b} = 60, 8.5$ ms [7], $C_b = 50$ s⁻¹, $M_{b0} = 0.33$ M and $M_{a0} = 100$ M, where C is the exchange rate, M is the proton concentration and a and b refer to the water and amide pool, respectively. Z-spectra generated using these three methods were plotted to assess their differences.

Phantom study: Tissue like creatine phantoms were prepared with concentrations of 100 and 125 mM, and three different pH values: 5.5, 6.0 and 6.5. PC was applied to the phantoms using a 4.7 T DirectDrive™ spectrometer (Agilent Technologies,

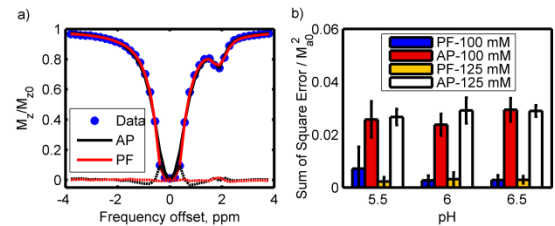


Fig. 2a) Fitted spectra for 125 mM creatine phantoms at pH 6.5; b) fitted errors using AP approximation and PF. The lines below the z-spectra in a) are the residual plots.

Results: Fig. 1 shows the simulated spectra from PC and those obtained using the AF and AP approximations. AF is not a suitable approximation as it under-estimates the saturation of the water pool, the AP generated z-spectrum matched well with that from PC, except at the frequency offsets near ω_a and chemical shift of amide protons (1.9 ppm). Fig. 2a shows the acquired CEST data and the fits using PF and the AP approximation. From the residual plots, PF fitted well to the measured data, the AP method also produced good fits, except at the offsets near ω_a – reproducing the results found in the simulations. The fitted errors to the measured data using different methods are plotted in Fig. 2b; PF errors were much lower than the AP approximation fitted errors. Fig. 3 is the fitted ω_a using PF and AP approximation, good agreement was found. Fig. 4 shows the fitted C_b values which were correlated to the pH of the phantoms as expected. No significant difference was found for a two-tailed t-test at 5 % significant level. Nevertheless, the standard deviation of the fitted C_b using PF is lower for the high pH phantoms.

Discussion: Although PF was able to fit better than the AP approximation, the smaller fitted errors of the former did not translate to better quantification of ω_a and C_b . Thus, AP approximation, which is much faster to compute than the PF, appears to be suitable for fitting measured CEST data that have small C_b such as that found in amide proton transfer imaging. When an optimal sampling schedule